EGFR activation coupled to inhibition of tyrosine phosphatases causes lateral signal propagation

Andrew R. Reynolds*†, Christian Tischer‡†, Peter J. Verveer‡, Oliver Rocks‡§ and Philippe I. H. Bastiaens‡¶

*Cell Biophysics Laboratory, Cancer Research UK London Research Institute, Lincoln's Inn Fields Laboratories, 44 Lincoln's Inn Fields, London WC2A 3PX, UK

‡European Molecular Biology Laboratory, Meyerhofstrasse 1, 69117 Heidelberg, Germany

§Max-Planck-Institute for Molecular Physiology, Otto-Hahn-Strasse 11, 44227 Dortmund, Germany

†These two authors contributed equally to this work

¶e-mail: bastiaen@embl-heidelberg.de

Published online: 22 April 2003; DOI: 10.1038/ncb981

The epidermal growth factor receptor (EGFR) belongs to the receptor tyrosine kinase (RTK) superfamily and is involved in regulating cell proliferation, differentiation and motility[1]. Growth factor binding induces receptor oligomerization at the plasma membrane[2–5], which leads to activation of the intrinsic RTK activity and *trans*-phosphorylation of tyrosine residues in the intracellular part of the receptor[6,7]. These residues are docking sites for proteins containing Src homology domain 2 and phosphotyrosine-binding domains that relay the signal inside the cell[8–10]. In response to EGF attached to beads, lateral propagation of EGFR phosphorylation occurs at the plasma membrane[11], representing an early amplification step in EGFR signalling. Here we have investigated an underlying reaction network that couples RTK activity to protein tyrosine phosphatase (PTP) inhibition by reactive oxygen species. Mathematical analysis of the chemical kinetic equations of the minimal reaction network detects general properties of this system that can be observed experimentally by imaging EGFR phosphorylation in cells. The existence of a bistable state in this reaction network explains a threshold response and how a high proportion of phosphorylated receptors can be maintained in plasma membrane regions that are not exposed to ligand.

Inhibition of PTPs by phenylarsineoxide (PAO; Supplementary Information, Fig. S1a), pervanadate or α-bromo-4-hydroxyacetophenone (data not shown) was sufficient to induce rapid phosphorylation of EGFR fused to green fluorescent protein (EGFR–GFP). This corroborates the idea that the overall state of receptor phosphorylation in quiescent cells is the net result of basal RTK and PTP activities[12]. Hydrogen peroxide also induces rapid phosphorylation of EGFR[13], most probably by a transient inhibition of PTP mediated by oxidation of the catalytic cysteine thiolate to a sulphenic acid[14,15]. Because hydrogen peroxide is produced rapidly after growth factor stimulation by enzyme systems such as nicotinamide adenine dinucleotide phosphate (NADPH) oxidase[16], we investigated whether ligand-independent propagation of EGFR signals is mediated by the diffusion of hydrogen peroxide. In this scheme, enzymatic hydrogen-peroxide-scavenging systems such as catalase should prevent the amplification of EGFR phosphorylation at the plasma membrane.

The microinjection of cells with a catalase cDNA abolished phosphorylation spreading in more than 50% of MCF7 cells that had been stimulated with EGF attached to beads (EGF-beads; Fig. 1a). The bimodal distribution of responding and nonresponding cells implies that in a single cell the phosphorylation propagation response behaves as a switch that depends on the expression level of catalase. Control cells that did not express catalase all amplified receptor phosphorylation after bead stimulus (Fig. 1a, b).

We also observed rapid phosphorylation of EGFR–GFP in MCF7 cells treated with hydrogen peroxide (Fig. 1c); however, phosphorylation was extended to receptors on endo-membranes (Fig. 1c; Supplementary Information, Fig. S2), showing that PTP activity also maintains low phosphorylation of EGFR in these internal membranes. Phosphorylation of EGFR–GFP in endo-membranes was not observed when cells were stimulated with EGF or EGF-beads (Fig. 1d and Supplementary Information, Fig. S2), indicating that reactive oxygen species (ROS) produced after growth factor stimulation are spatially constrained to a layer below the plasma membrane.

To investigate the role of ligand-independent EGFR kinase activity on receptor phosphorylation, we stimulated cells expressing a kinase-dead mutant of EGFR fused to green fluorescent protein ($EGFR^{V741G}$–GFP)[17] with hydrogen peroxide. On the timescale of phosphorylation spreading (< 5 min), phosphorylation of the stimulated mutant EGFR was comparable to that in quiescent cells (Fig. 1c, d). This shows that the kinase activity of EGFR is necessary for propagating phosphorylation mediated by hydrogen peroxide. Note that MCF7 cells express small quantities of endogenous EGFR, which are probably responsible for the slight increase in phosphorylation of $EGFR^{V741G}$–GFP observed at longer time points (15 min). Taken together, these results indicate that a mechanism relying on PTP inhibition coupled to RTK activation is responsible for spreading phosphorylation to non-ligand-bound EGFR receptors.

To investigate the implications of a coupling between PTP and RTK activity in more detail, we formulated and analysed the minimal reaction network shown in Fig. 2a. We do not consider this model to be a definitive description of the complete reaction network in the cell, but it allows us to understand the general capabilities of such a feedback system and to devise experiments to test these.

Receptor phosphorylation was modelled as a bimolecular reaction between receptors, where the basal kinase activity (α_1) is enhanced by a factor α_2/α_1 on phosphorylation of the receptor. Receptor dephosphorylation is catalysed by active PTPs. The rate of PTP inhibition was modelled to be proportional to the amount of phosphorylated receptor, assuming that this is the principal molecular species that couples to the ROS production pathway. Oxidation of the catalytic cysteine thiolate in PTPs is reversible (k_4; Fig. 2a)[14]. For simplicity, we assumed the rate of PTP reactivation to

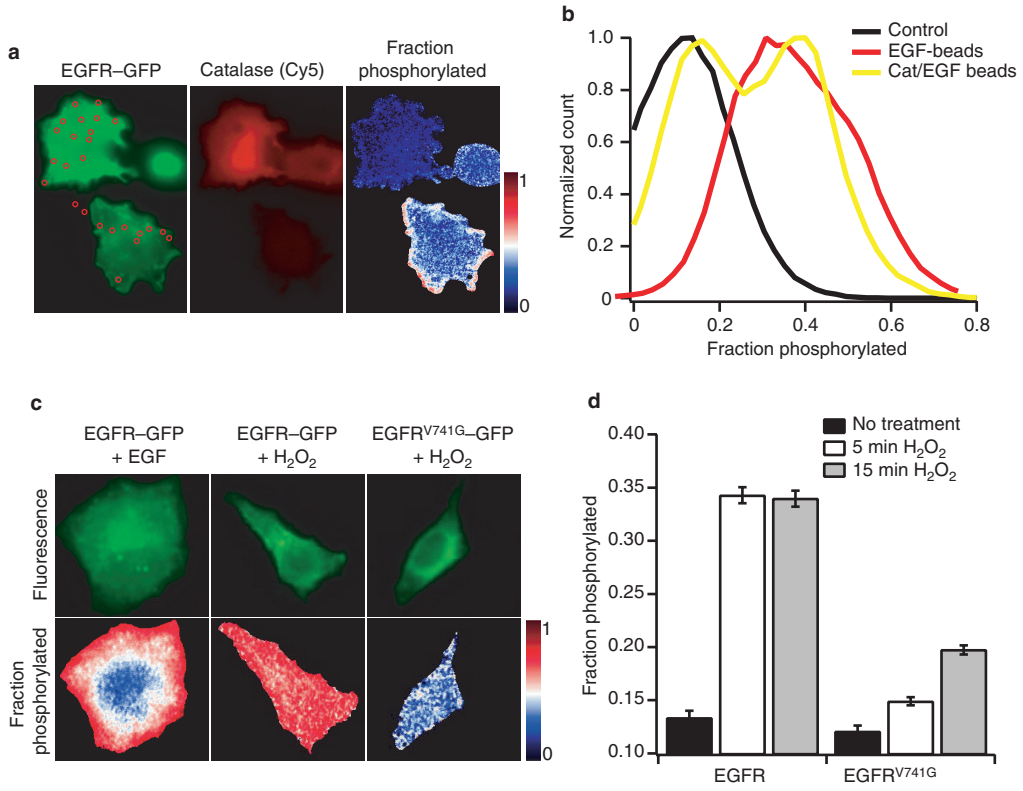

Figure 1 **Hydrogen peroxide enables EGFR lateral phosphorylation propogation.** **a**, Expression of catalase inhibits EGF-bead-induced lateral propogation of EGFR–GFP phosphorylation. MCF7 cells were microinjected with a plasmid encoding human fibroblast catalase and stimulated with EGF-beads for 2 min. Left, EGFR–GFP fluorescence (green) and EGF-beads (red circles); middle, anti-catalase staining; right, phosphorylated receptor population. **b**, Phosphorylated EGFR–GFP populations. Control, nonstimulated cells (n = 10); EGF-beads, cells locally stimulated with EGF-beads for 2 min (n = 8); cat/EGF-beads, catalase-expressing cells locally stimulated with EGF-beads (n = 10). **c**, Distribution of EGFR–GFP phosphorylation in MCF7 cells after treatment with EGF or hydrogen peroxide. Top row, EGFR–GFP fluorescence. Bottom row, populations of phosphorylated receptors. Left, stimulation with 100 ng ml^{-1} EGF for 2 min; middle, stimulation with 4 mM hydrogen peroxide for 2 min; right, stimulation of MCF7 cells expressing kinase-dead EGFR^{V471G}–GFP with 4 mM hydrogen peroxide for 2 min. **d**, Average populations of phosphorylated wild-type and kinase-dead EGFR–GFP after treatment with 4 mM hydrogen peroxide quantified by global analysis of FLIM data (n = 20 cells per data point). EGFR, MCF7 cells expressing EGFR–GFP; EGFR^{V471G}, MCF7 cells expressing EGFR^{V471G}–GFP.

be constant as we are not aware of a modulation of enzyme activities that can catalyse this reaction.

The reaction network was transformed into chemical kinetic equations that were solved for the steady states in the absence of a stimulus (see Methods). Given that uncatalysed reactions are negligible, we found that the steady states are determined by three effective parameters: (1) the enhancement of kinase activity on receptor phosphorylation (α_2/α_1); (2) the ratio of maximal phosphatase activity to maximal kinase activity ($P/K = [\mathrm{PTP}]_{tot}\gamma k_2/([\mathrm{RTK}]_{tot}\alpha_2 k_1)$); and (3) the ratio of the maximal rate of phosphatase inhibition to the rate of phosphatase reactivation ($I/R = [\mathrm{RTK}]_{tot}\beta k_3/k_4$).

Depending on these parameters the system operates in one of three possible modes: (1) a single, stable steady state at low phosphorylation of receptor; (2) a single, stable steady state at high phosphorylation of receptor; or (3) a bistable state. In the bistable state, phosphorylation of the receptor can be either high ('activated') or low ('resting'), depending on the starting conditions (refs 18, 19 and Fig. 2c).

In such bistable systems, a local perturbation (such as ligand stimulation) can lead to the formation of a reaction wavefront that propagates the transition from the resting to the activated state[20]. Local cycles of EGFR activation, hydrogen peroxide production and PTP inhibition can propagate along the plasma membrane. This does not require the long-range diffusion of a transmitter molecule such as hydrogen peroxide but is mediated by local interactions of diffusing proteins such as the *trans*-autoactivation of EGFRs by transient dimer formation[21]. This mechanism could explain how local production of hydrogen peroxide mediates phosphorylation propagation at the plasma membrane without triggering the phosphorylation of receptors on endo-membranes.

We investigated which system settings allow bistability and determined the following minimal requirements for each parameter: (1) the rate of maximal phosphatase inhibition exceeds the rate of phosphatase reactivation ($I/R > 1$); (2) kinase activity of the receptor increases on phosphorylation ($\alpha_2 > \alpha_1$); and (3) the maximal PTP activity is greater than the maximal kinase activity ($P/K > 1$). Published work indicates that these conditions are fulfilled: the rate of PTP inhibition by hydrogen peroxide has been measured to be 10–100 times faster than the rate of reactivation[14], the catalytic activity of RTKs has been reported to be 3–100 times greater upon phosphorylation[21–23], and the catalytic activity of PTPs is typically 10–1,000 times higher than that of RTKs[24]. If the above conditions are met, a proper balance of all parameters yields bistability.

According to our model, propagation of phosphorylation is only possible in the bistable regime of the reaction network. If all other parameters are kept constant, an increase in receptor expression can shift the system from the 'stable' to the 'bistable' or even the 'constitutively active' mode (Fig. 2b). This theoretical finding is in good agreement with a experimental study in which activation of Ras and phosphorylation of CrkII was monitored by GFP-based

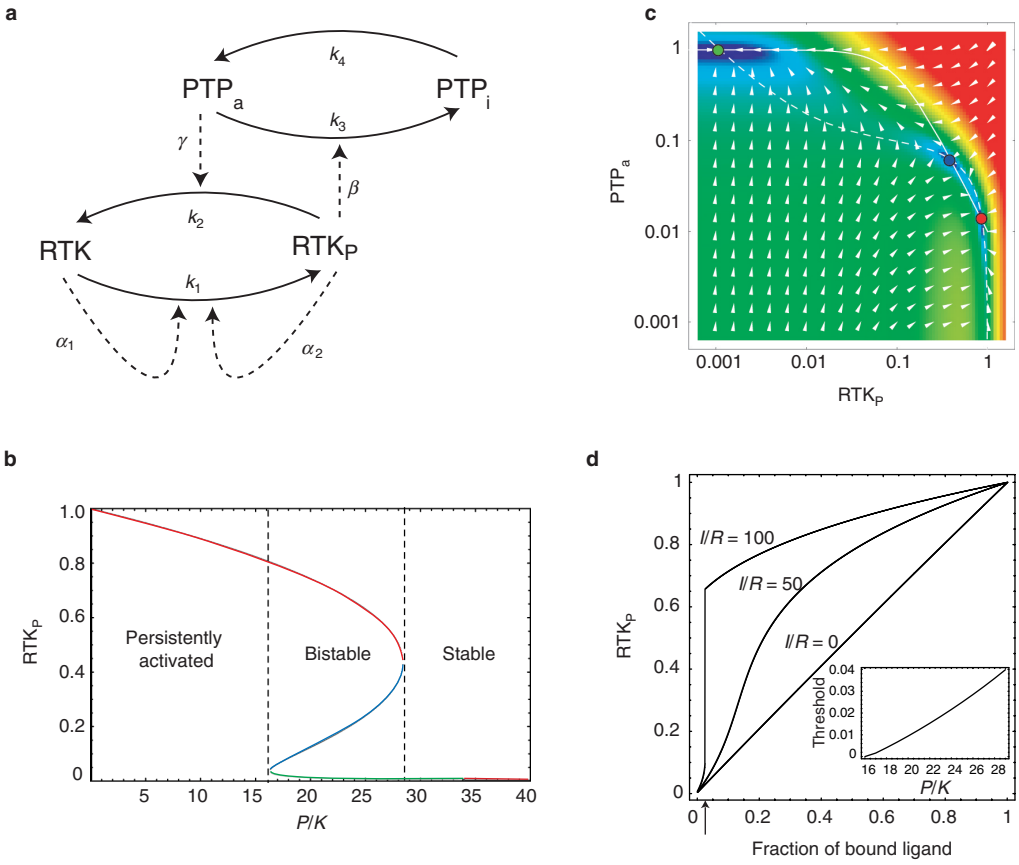

Figure 2 **Analysis of the RTK and PTP reaction network. a**, Reaction network scheme showing the coupling of PTP inhibition and RTK activation. Unbroken arrows represent a reaction that causes the transition of a molecule between two states (PTP, active–inactive; RTK, phosphorylated–unphosphorylated). Broken arrows indicate catalysis. **b**, Calculated fraction of phoshorylated RTK (RTK_P) at steady states as a function of the relative maximal PTP to RTK activity (P/K). Green and red lines, stable steady states ('resting' and 'activated', respectively); blue lines, unstable saddle point. Where the red and green lines coincide, the system is bistable. Parameters: $I/R = 100$; $\alpha_2/\alpha_1 = 10$. **c**, State space scheme in the bistable regime. At each point in the plane, the reaction kinetics determines how fast (red, fast; blue, slow) and in which direction (arrow) the state is changing. With this scheme, the response of the system to any initial condition can be predicted by following the arrows. On the unbroken curve there is no initial change in PTP activity (horizontal arrows); on the broken curve there is no initial change in RTK phosphorylation (vertical arrows). Where the curves intersect, there are steady-state solutions. Two steady-state solutions are stable against small perturbations, because all arrows in their vicinity point towards the intersections. The two stable steady states are at high (low) PTP activity and low (high) RTK phosphorylation (green and red circle, respectively). There is one unstable saddle point (blue circle). Parameters: $I/R = 100$; $\alpha_2/\alpha_1 = 10$; $P/K = 25$. **d**, Calculated dose–response curves. The fraction of phosphorylated receptors (RTK_P) is plotted against the fraction of ligand-bound receptors for different coupling of PTP inhibition to RTK activation. For strong coupling ($I/R = 100$), the system is in the bistable regime and shows a step-like response to a threshold concentration of ligand-bound receptors (arrow). For no coupling ($I/R = 0$) there is a linear response, whereas for intermediate coupling ($I/R = 50$) there is initial amplification but no step. Parameters: $\alpha_2/\alpha_1 = 10$; $P/K = 25$. Inset shows the relation of threshold density of ligand-bound receptor (arrow in main figure) versus the relative PTP to RTK activity (P/K) for values in the bistable regime (compare **b**). Parameters: $I/R = 100$; $\alpha_2/\alpha_1 = 10$.

sensors in cells that were subjected to a laminar flow of rhodamine-tagged EGF[25]: only local EGFR activation occurred in Cos cells expressing $3–5 \times 10^4$ endogenous receptors, but a 2–3-fold increase in receptor expression over endogenous levels resulted in lateral propagation of the signal[25].

We also tested whether phosphorylation spreading occurs at low levels of endogenous receptor expression by imaging the activation of Harvey Ras (HRas) after local EGFR stimulation in Madin–Darby canine kidney (MDCK) cells (Supplementary Information, Fig. S3). Unexpectedly, a substantial population of cells showed delocalized activation of HRas after a local stimulus; this suggests that lateral signal propagation still occurs at low levels of receptor expression because active HRas–GTP colocalizes with activated EGFR[25]. These results indicate that other parameters, such as P/K and I/R, should be also considered when comparing different types of cell for their ability to propagate EGFR phosphorylation.

But does ligand presentation on beads facilitate phosphorylation propagation at low receptor expression? In comparison to soluble stimuli, ligand presentation on a solid support inhibits rapid endocytosis and could increase the concentration of receptors above the average density in the membrane (provided that the ligand density is higher than the average receptor density). Stimulus by a ligand on a solid support therefore could result in a prolonged high concentration of activated receptors. Locally, this could overcome the threshold required for initiating phosphorylation propagation. These effects would apply only to the membrane area below the bead, however, and receptor concentration or endocytosis outside this region would not be affected directly. The ability of the cell to maintain a high number of phosphorylated receptors in unstimulated membrane areas is a general property of the proposed RTK–PTP feedback system and is independent of the specific stimulus that triggers transition to the activated state. Bead-bound

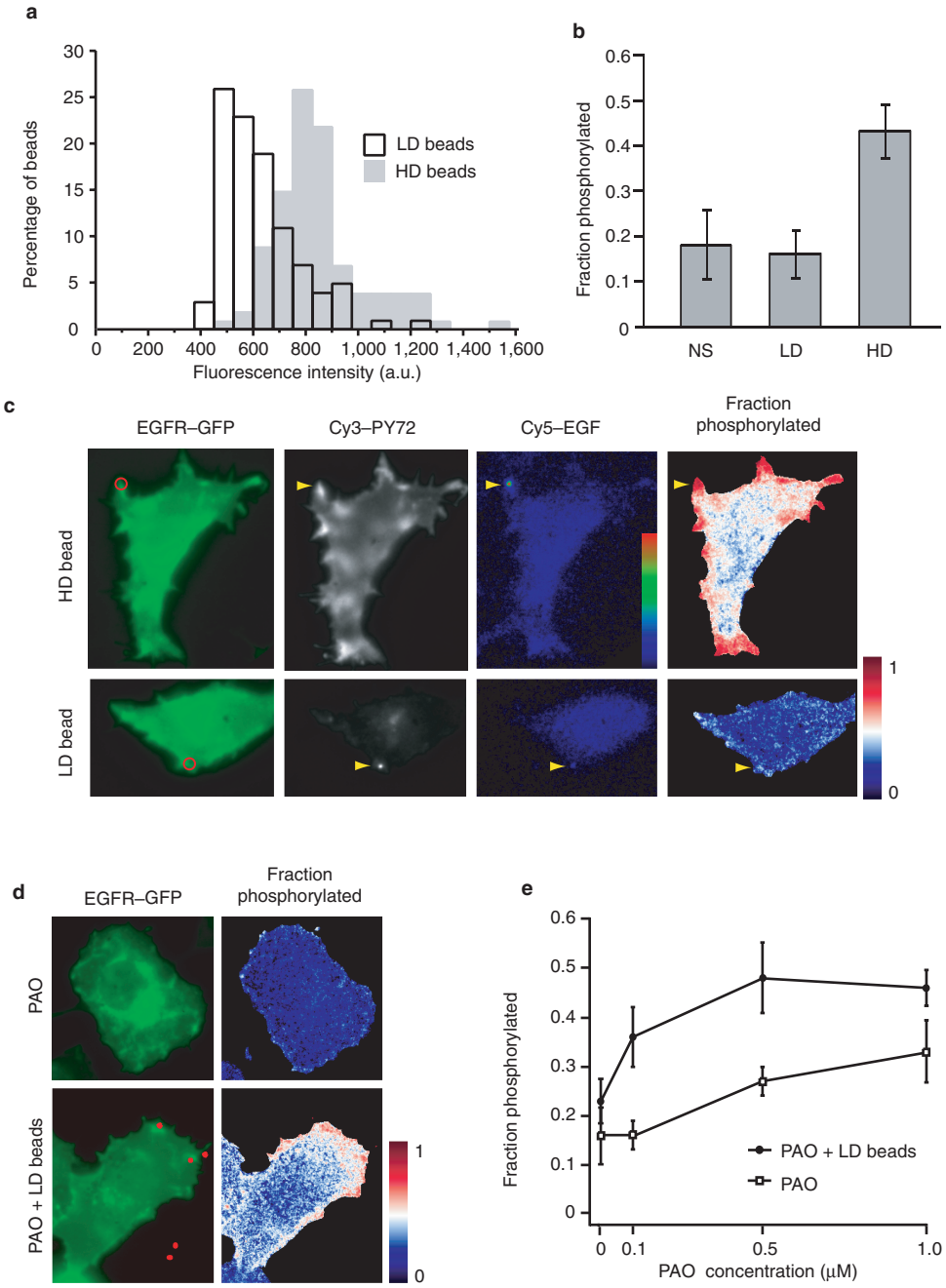

Figure 3 **Threshold response of phosphorylation propagation. a**, Relative density of EGF coupling to beads quantified by anti-EGF immunofluorescence staining. Beads coupled to EGF in the absence of Tris buffer stained more brightly (HD-beads) than did beads coupled in the presence of Tris buffer (LD-beads). **b**, Average populations of phosphorylated EGFR–GFP detected in nonstimulated (NS) cells (n = 13) or cells stimulated for 5 min with LD-beads (n = 5) or HD-beads (n = 13). **c**, MCF7 cells expressing EGFR–GFP were stimulated for 2 min with beads with high (HD-bead) or low (LD-bead) surface densities of coupled EGF. Left, EGFR–GFP fluorescence (green) and EGF-beads (red circles); middle left, Cy3–PY72 staining; middle right, anti-EGF staining; right, phosphorylated receptor populations. Arrowheads indicate bead contact points. **d**, Representative examples of MCF-7 cells expressing EGFR–GFP incubated with 0.1 μM PAO or 0.1 μM PAO plus LD-beads. Left, EGFR–GFP fluorescence (green) and LD-beads (red); right, phosphorylated receptor populations. **e**, Average populations of phosphorylated receptors measured from cells incubated with different concentrations of PAO in the presence (filled circles) or absence (open squares) of LD-beads (~10 cells per data point).

receptors can therefore trigger the amplification mechanism locally, but if the parameter settings of the reaction network outside this area cannot sustain high numbers of phosphorylated receptors (for example, owing to low receptor density), the signal will not propagate.

To calculate the response to a stimulus, we modelled the system further by introducing constitutively activated ligand-bound receptors that cannot be deactivated by phosphatases[12], which effectively amounts to an increase in kinase activity on ligand binding. Figure 2d shows the calculated dose–response curves for different values of I/R with constant values of the other parameters. When I/R equals zero, there is no inhibition of PTPs induced by the activated receptors and the fraction of phosphorylated receptors is a continuous

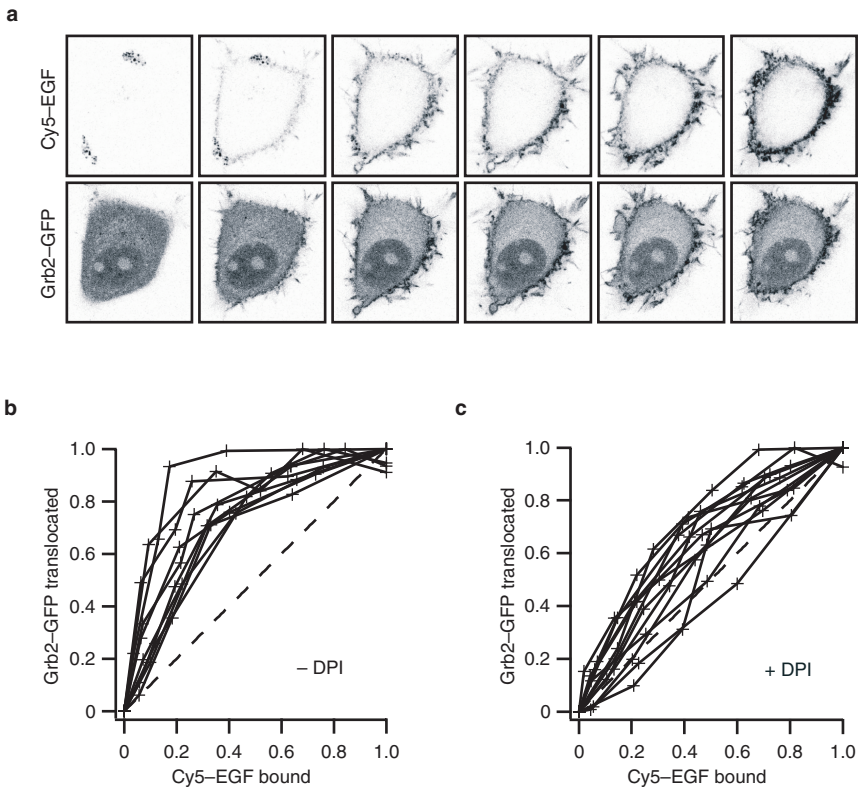

Figure 4 **EGF dose–response of EGFR-expressing MCF7 cells. a**, Series of confocal fluorescence images of Grb2–GFP and Cy5–EGF. After each scan, 4 ng ml^{-1} Cy5–EGF was added and allowed to bind for 2 min before the next image was taken. **b**, Quantification of Grb2 translocation as a function of total Cy5–EGF binding (n = 10 cells). **c**, Cells were incubated with 10 μM DPI for 30 min before the first stimulation (n = 13 cells).

function of ligand binding (that is, a graded response). For a strong coupling (high I/R), the system operates in the 'bistable regime' and responds as a switch: above a threshold concentration of ligand, the system 'jumps' from the resting into the activated state.

To test experimentally predictions of the response analysis, we first assessed the network in its unperturbed state. Pharmacological agents were then examined for their ability to change the parameter settings of the system. Finally, the system response after perturbation with pharmacological agents was compared with the theoretical predictions.

Analysis of the coupled RTK–PTP network indicated that signal amplification depends on a threshold density of ligand-bound receptor. To test this, we coupled EGF to beads at two densities differing on average by a factor of two, denoted high density (HD)-beads and low-density (LD)-beads (Fig. 3a). Cells stimulated with LD-beads showed increased anti-phosphotyrosine staining only at the bead contact point, whereas HD-beads resulted in an increase in phosphorylated EGFR across the whole plasma membrane (Fig. 3b, c). This observation shows that a threshold density of EGF is indeed needed to trigger phosphorylation propogation. At the average expression of EGFR–GFP (2×10^5 receptors per cell), we did not observe an increased density of receptors below HD-beads (Figs 1a and 3c), indicating that this was not the trigger of propagation.

In theory, the ligand threshold at which amplification occurs should decrease as the net kinase activity in the cell increases (corresponding to a decrease in P/K; Fig. 2d, inset). This can be achieved experimentally by lowering the activity of the PTPs that maintain the low phosphorylation state of EGFR in the absence of stimulus. Because these PTPs are not yet identified, we used PAO as generic PTP inhibitor and confirmed its effect on net kinase activity (Supplementary Information, Fig. S1a). Cells were pre-incubated for 2 min with PAO and then stimulated for 2 min with LD-beads in the continued presence of PAO. Under these conditions, phosphorylated receptors appeared across the whole plasma membrane (Fig. 3d, e). The average populations were significantly higher than in control cells, which were treated with the same PAO concentration for an equivalent time but not stimulated. The required density of EGF on beads for initiating spreading was therefore lower in the presence of PTP inhibitor, as predicted by our analysis.

The analysis also shows that a strong coupling of PTP inhibition to RTK activation leads to high phosphorylation of receptors already at a low density of bound ligand (Fig. 2d). We therefore investigated the response of single, live MCF7 cells transfected with EGFR to stimulation with soluble ligand. Receptor phosphorylation was monitored by the translocation of Grb2–GFP to the plasma membrane, and ligand binding by imaging Cy5-labelled EGF (Cy5–EGF). We added Cy5–EGF in stepwise doses with 2 min between successive additions to allow Grb2 translocation to complete (Supplementary Information, Fig. S1b). A very steep dose–response curve was observed in which the main portion of Grb2–GFP translocated when approximately 20% of the receptors were bound to ligand. Increased addition of Cy5–EGF led to further binding to the receptors with little or no increase in Grb2–GFP translocation (Fig. 4a, b).

According to our model, the amplification of receptor phosphorylation at low doses of EGF is weaker if the coupling of RTK activation to PTP inhibition is reduced, corresponding to a shift of the

system to the 'stable' state (Fig. 2d). We found that this could be reliably achieved by reducing the amount of produced ROS with the NADPH oxidase inhibitor diphenyleneiodonium (DPI)[26], which abolished phosphorylation propagation in all cases (Supplementary Information, Fig. S4). Indeed, pre-incubating cells for 30 min with DPI resulted in the predicted more linear phosphorylation response to homogenous ligand stimulation (Fig. 4c).

In conclusion, we have investigated the implications of a coupling between RTK activation and PTP inhibition by hydrogen peroxide. Such a coupling adds a feedback loop to the control of RTK phosphorylation. In agreement with theoretical analysis, quantitative imaging of EGFR phosphorylation indicated that such a reaction network can respond in a highly amplified and switch-like manner to a threshold concentration of ligand stimulus. We have also shown how the response of the reaction network can be modified by changes in the system parameters induced by pharmacological agents. The identification and quantitative analysis of such feedback systems will complement our picture of linear signalling pathways. □

Methods

Cell culture

MCF7, Cos7 and MDCK cells were routinely maintained in DMEM medium supplemented with 10% foetal calf serum (FCS). For live cell microscopy experiments, we transferred cells to low bicarbonate DMEM medium without phenol red supplemented with 25 mM HEPES buffer (pH 7.4).

Cell transfection, EGF stimulation and drug treatment

The transient expression of GFP-tagged proteins was achieved by transfecting cells with plasmid DNA using the Fugene reagent (Roche, Basel, Switzerland). For ROS scavenging experiments, we microinjected MCF7 cells expressing EGFR–GFP with 200 μg ml^{-1} of an expression plasmid encoding human fibroblast catalase (a gift from J. Melendez) and allowed the cells to express for at least 20 h before stimulation. Transfected cells were serum-starved for 5–6 h before all experiments. Focal stimulation with EGF-beads was done as described[11].

A 30% solution of hydrogen peroxide (Calbiochem, San Diego, CA) was pre-diluted in PBS before its application to cells. PAO (Calbiochem) was dissolved first in water and then in media to achieve the appropriate concentration. We pre-diluted DPI (Sigma, St Louis, MO) to 0.2 mM in PBS from a 10 mM stock solution in dimethylsulphoxide. The pre-diluted DPI was added to serum-starved MCF7 cells at a final concentration of 10 μM. The cells were incubated for 30 min before stimulation with growth factor or beads.

Fixation and immunocytochemistry

After treatment with growth factors and/or drugs, cells were fixed with 4% paraformaldehyde (PFA) at room temperature for 20 min. We washed cells briefly with 100 mM Tris (pH 7.4) and 50 mM NaCl, permeabilized them with 0.1% Triton X-100 in PBS for 10 min, and then stained them for 60 min with a Cy3-conjugated antibody against phosphotyrosine (PY72; Cancer Research UK, London). In some experiments, cells were co-stained for EGF or catalase using, respectively, a rabbit polyclonal antibody against either mouse EGF (Sigma) or human erythrocyte catalase (Calbiochem) and visualized with Cy5-conjugated goat antibodies against rabbit IgG (Jackson Immunoresearch Laboratories). We mounted the coverslips on glass slides in Mowiol solution (Calbiochem) for microscopy.

Coupling of EGF to beads

Mouse submaxillary gland EGF was obtained as a residue lyophilized from 15 mM acetic acid (Calbiochem). Carboxylate-modified, 0.8-μm diameter latex beads (Sigma) were derivatized with *N*-hydroxysuccinimde ester groups as described[11]. We divided the beads in half, resuspended each half in 10 μM EGF, 65 mM acetic acid and 150 mM bicine (pH 8.3; either supplemented or not with 10 μM Tris) and left them to react for 2 h at room temperature. We terminated the coupling reaction by adding hydroxylamine at a final concentration of 10 mM. Free EGF was removed from the coupling reaction by five washes with PBS. The EGF-beads were resuspended in a 1:1 solution of glycerol and PBS and stored at −20 °C.

Alternatively, 0.4 mg of dry volume streptavidin latex beads (diameter 1.0 μm, Sigma) was incubated with 12 μl of an aqueous 0.1 μg $μl^{-1}$ solution of biotin-conjugated EGF (Molecular Probes, Eugene, OR) in a total aqueous volume of 200 μl for 2 h at 4 °C under rotation. Free biotin–EGF was removed by five washes with PBS, followed by dialysis against an excess of avidin (Molecular Probes) in PBS for 24 h at 4 °C. We then washed the beads in PBS and resuspended them in 100 μl of a 1:1 solution of glycerol and PBS. The beads were used on the day of preparation. For control experiments, streptavidin beads were treated in parallel in exactly the same manner with unmodified EGF. Ras activation was not observed with a high concentration of control beads or when the supernatant from the final washing step of biotin–EGF bead preparation was used.

Quantification of EGF density on beads

Poly-L-lysine coated glass coverslips were incubated with 30 μl of EGF-beads diluted in PBS (~1×10^6 beads) for 3 h at 4 °C, and then fixed with 4% PFA to immobilize the beads. We stained the coverslips with antibodies against mouse EGF (1:10,000 dilution in 1% bovine serum albumin in PBS), followed by Cy3-conjugated goat antibodies against rabbit IgG, and then mounted the coverslips on glass slides in Mowiol solution. Cy3 fluorescence images were taken using a standard epifluorescence microscope and the average fluorescence intensity of individual beads was quantified.

Microscopy

Fluorescence lifetime imaging microscopy (FLIM) sequences were obtained at a modulation frequency of 80 MHz with an Olympus IX70 microscope, using a 100×/1.4 NA oil objective immersion lens. Cyan fluorescent protein (CFP) and GFP were excited by the 457.9-nm and 476-nm argon laser lines, respectively. Fluorescence was detected with a dichroic beamsplitter (Q495 LP; Chroma Technology, Brattleboro, VT) and a narrow-band emission filter (HQ510/20; Chroma) for GFP, and a dichroic beamsplitter (467; DELTA, Lyngby, Denmark) and a narrow-band emission filter (HQ480/20; Chroma) for CFP. The Cy3 images were recorded using a 100-W mercury arc lamp with a high Q Cy3 filter set (excite, HQ545/30; dichroic, Q580 LP; emitter, HQ610/75). We analysed FLIM data by global analysis software as described[11,27].

Confocal laser scanning microscopy was done on a Leica TCS SP2 (Leica, Wetzlar, Germany) or LSM510 (Zeiss, Jena, Germany), which were both equipped with a 63×/1.3 NA oil immersion lens. We excited CFP, GFP and yellow fluorescent protein (YFP) by the 457.9-nm, 488-nm and 514-nm argon laser lines, respectively. Cy3 and Cy5 were excited by the 543-nm and 633-nm HeNe laser lines, respectively.

For the Grb2–GFP translocation experiments, GFP and Cy5 were scanned simultaneously by the 488-nm and 633-nm laser lines. Grb2–GFP translocation was quantified by the depletion of fluorescence from the cytosol, because rapid diffusion assures that the fluorescence intensity in a cytosolic region is a reliable readout of the remaining average concentration. To determine the amount of bound ligand, we integrated the fluorescence of Cy5–EGF on the plasma membrane.

Modelling of the reaction network

Using the material balances:

$$[PTP]_{tot} = [PTP_a] + [PTP_i] \quad (1)$$

$$[RTK]_{tot} = [RTK] + [RTK_P] \quad (2)$$

the reaction network shown in Fig. 2a transforms into the following differential equations that govern the quantities of phosphorylated RTKs and active PTPs:

$$\partial_t[RTK_P] = ([RTK]_{tot} - [RKT_P])(k_1\alpha_1([RTK]_{tot} - [RTK_P]) + k_1\alpha_2[RTK_P]) - k_2\gamma[RTK_P][PTP_a] \quad (3)$$

$$\partial_t[PTP_a] = k_4([PTP]_{tot} - [PTP_a]) - k_3\beta[RTK_P][PTP_a] \quad (4)$$

Steady states were calculated by setting the derivatives in equations (3) and (4) to zero.

RECEIVED 6 SEPTEMBER 2002; REVISED 20 DECEMBER 2002; ACCEPTED 4 MARCH 2003; PUBLISHED 22 APRIL 2003.

1. Schlessinger, J. Cell signaling by receptor tyrosine kinases. *Cell* **103,** 211–225 (2000).
2. Mohammadi, M. *et al.* Aggregation-induced activation of the epidermal growth factor receptor protein tyrosine kinase. *Biochemistry* **32,** 8742–8748 (1993).
3. Yarden, Y. & Schlessinger, J. Epidermal growth factor induces rapid, reversible aggregation of the purified epidermal growth factor receptor. *Biochemistry* **26,** 1443–1451 (1987).
4. Cochet, C. *et al.* Demonstration of epidermal growth factor-induced receptor dimerization in living cells using a chemical covalent cross-linking agent. *J. Biol. Chem.* **263,** 3290–3295 (1988).
5. Zhou, M. *et al.* Real-time measurements of kinetics of EGF binding to soluble EGF receptor monomers and dimers support the dimerization model for receptor activation. *Biochemistry* **32,** 8193–8198 (1993).
6. Yarden, Y. & Schlessinger, J. Self-phosphorylation of epidermal growth factor receptor: evidence for a model of intermolecular allosteric activation. *Biochemistry* **26,** 1434–1442 (1987).
7. Honegger, A. M., Kris, R. M., Ullrich, A. & Schlessinger, J. Evidence that autophosphorylation of solubilized receptors for epidermal growth factor is mediated by intermolecular cross-phosphorylation. *Proc. Natl Acad. Sci. USA* **86,** 925–929 (1989).
8. Alroy, I. & Yarden, Y. The ErbB signaling network in embryogenesis and oncogenesis: signal diversification through combinatorial ligand-receptor interactions. *FEBS Lett.* **410,** 83–86 (1997).
9. Pawson, T. Non-catalytic domains of cytoplasmic protein-tyrosine kinases: regulatory elements in signal transduction. *Oncogene* **3,** 491–495 (1988).
10. Kavanaugh, W. M. & Williams, L. T. An alternative to SH2 domains for binding tyrosine-phosphorylated proteins. *Science* **266,** 1862–1865 (1994).
11. Verveer, P. J., Wouters, F. S., Reynolds, A. R. & Bastiaens, P. I. H. Quantitative imaging of lateral ErbB1 receptor signal propagation in the plasma membrane. *Science* **290,** 1567–1570 (2000).
12. Ostman, A. & Bohmer, D. Regulation of receptor tyrosine kinase signaling by protein tyrosine phosphatases. *Trends Cell Biol.* **11,** 258–266 (2001).
13. Gamou, S. & Shimizu, N. Hydrogen peroxide preferentially enhances the tyrosine phosphorylation of epidermal growth factor receptor. *FEBS Lett.* **357,** 161–164 (1995).
14. Denu, J. M. & Tanner, K. G. Specific and reversible inactivation of protein tyrosine phosphatases by hydrogen peroxide: evidence for a sulfenic acid intermediate and implications for redox regulation. *Biochemistry* **37,** 5633–5642 (1998).
15. Meng, T. C., Fukada, T. & Tonks, N. K. Reversible oxidation and inactivation of protein tyrosine phosphatases *in vivo*. *Mol. Cell* **9,** 387–399 (2002).
16. Finkel, T. Oxygen radicals and signaling. *Curr. Opin. Cell Biol.* **10,** 248–253 (1998).
17. Groenen, L. C., Walker, F., Burgess, A. W. & Treutlein, H. R. A model for the activation of the epidermal growth factor receptor kinase involvement of an asymmetric dimer? *Biochemistry* **36,** 3826–3836 (1997).
18. Ferrell, J. E. Self-perpetuating states in signal transduction: positive feedback, double-negative feedback and bistability. *Curr. Opin. Cell Biol.* **14,** 140–148 (2002).
19. Tyson, J. J., Chen, K. & Novak, B. Network dynamics and cell physiology. *Nature Rev. Mol. Cell Biol.* **2,** 908–916 (2001).
20. Murray, J. D. *Mathematical Biology* (Springer, Berlin, 1993).
21. Hubbard, S. R., Mohammadi, M. & Schlessinger, J. Autoregulatory mechanisms in protein tyrosine kinases. *J. Biol. Chem.* **273,** 11987–11990 (1998).
22. Bertics, P. J. & Gill, G. N. Self-phosphorylation enhances the protein-tyrosine kinase activity of the epidermal growth factor receptor. *J. Biol. Chem.* **260,** 14642–14647 (1985).
23. Hsu, C. Y., Hurwitz, D. R., Mervic, M. & Zilberstein, A. Autophosphorylation of the intracellular domain of the epidermal growth factor receptor results in different effects on its tyrosine kinase activity with various peptide substrates. *J. Biol. Chem.* **266,** 603–608 (1991).
24. Fischer, E. H., Charbonneau, H. & Tonks, N. K. Protein tyrosine phosphatases: a diverse family of intracellular and transmembrane enzymes. *Science* **253,** 401–406 (1991).

25. Sawano, A., Takayama, S., Matsuda, M. & Miyawaki, A. Lateral propagation of EGF signalling after local stimulation is dependent on receptor density. *Dev. Cell* **3,** 245–257 (2002).
26. Li, Y. & Trush, M. A. Diphenyleneiodonium, an NAD(P)H oxidase inhibitor, also potently inhibits mitochondrial reactive oxygen species production. *Biochem. Biophys. Res. Commun.* **253,** 295–299 (1998).
27. Verveer, P. J., Squire, A. & Bastiaens, P. I. H. Global analysis of fluorescence lifetime imaging microscopy data. *Biophys. J.* **78,** 2127–2137 (2000).

ACKNOWLEDGEMENTS
We thank K. Jalink for critically reading the manuscript; M. Offterdinger for the PTB–YFP construct; T. Zimmerman for technical help with movies; I. Yudushkin for DPI control experiments and E.-L. Florin for comments on the modelling. P.J.V. was supported by a Marie Curie Fellowship of the European Community.
Supplementary Information accompanies the paper on www.nature.com/naturecellbiology.
Correspondence and requests for materials should be addressed to P.I.H.B.

COMPETING FINANCIAL INTERESTS
The authors declare that they have no competing financial interests.